

## ***Supporting Information***

**for**

### **Kill two birds with one stone: Simultaneous removal of volatile organic compounds and ozone secondary pollution by a novel photocatalytic process**

**Yifan Sui<sup>1</sup>, Xiaohu Sun<sup>1</sup>, Jie Guan<sup>1</sup>, Zeqiu Chen<sup>1,\*</sup>, Xinjie Zhu<sup>1</sup>, Xiaoyi Lou<sup>2</sup>, Xiuli Li<sup>1</sup>, Jiaowen Shen<sup>1</sup>, Xiaomei Liu<sup>3</sup>, Xiaojiao Zhang<sup>1</sup>, Yaoguang Guo<sup>1,\*</sup>, Gangfeng Zhang<sup>4</sup>, Rui-Qin Zhang<sup>5</sup>**

*1 Shanghai Collaborative Innovation Centre for WEEE Recycling, School of Resources and Environmental Engineering, Shanghai Polytechnic University, Shanghai 201209, China*

*2 Laboratory of Quality Safety and Processing for Aquatic Product, East Sea Fisheries Research Institute, Chinese Academy of Fishery Sciences, Shanghai 200090, China*

*3 School of Mathematics, Physics and Statistics, Shanghai Polytechnic University, Shanghai 201209, China*

*4 Shanghai Academy of Environmental Sciences, Shanghai 200233, China*

*5 Department of Physics, City University of Hong Kong, Hong Kong SAR, 999077, China*

*\*: Corresponding Authors*

*E-mail: [zqchen@sspu.edu.cn](mailto:zqchen@sspu.edu.cn)(Z.Chen); [ygguo@sspu.edu.cn](mailto:ygguo@sspu.edu.cn) (Y. Guo)*

**6 Texts**

**11 Figures**

## **Text S1 Materials**

Magnesium oxide (MgO, CP) was from Shanghai Macklin Biochemical Co., Ltd., China. Ethanol (AR) was purchased from Shanghai Aladdin Biochemical Technology Co., Ltd., China. Melamine (CP), toluene (AR), ethyl acetate (AR), and proposed thin alumina (AR) were supplied by Sinopharm Chemical Reagent Co., Ltd., China. The chemicals of 5,5-dimethyl-1-pyrrolidine-N-oxide (DMPO, Sigma-Aldrich, > 97%) and 2,2,6,6-tetramethyl-4-piperidone (TEMP, Acros Organics, > 97% ) were used as the spin-trapping agents in the electron paramagnetic resonance (EPR) experiments. The trials utilized ultrapure water (18.2 M $\Omega$  · cm) as the water source, and the medications were immediately employed without any additional purification steps.

## **Text S2 CFD simulation**

CFD software was used to simulate the distribution of airflow and optical radiation inside the conventional and modified devices. The designed reactor is first modelled using Solidworks software, and then the established model is imported into Geometry of workbench for the abstraction of the fluid domain, after which the mesh software that comes with workbench is used for the mesh delineation, and finally it is imported into Fluent for the setup of the boundary conditions as well as the solution calculations. The boundary conditions are as follows: by default, the gas entering the cavity is pure air, the air pressure is 101.325 kPa, and the temperature is 298.15 K. The specified boundary type in workbench defines the inlet of the reactor as inlet, the outlet as outlet, the UV light as light, and the boundary of the reactor as wall, and the wind speed of the inlet of the fluid in Fluent is set to 2.4 m/s and outlet static pressure is 0. In exploring

the optimisation of the reactor simulation, the fluid defaulted to incompressible air and the density was set to 1.293 kg/m<sup>3</sup>.

Reactor light field simulation and parameter setting: Solidworks was used to build the model based on the actual conditions, the height of the UV lamp was 220 mm, the diameter was 19 mm, of which the light-emitting part of the UV lamp was 210 mm. The built model was imported into Geometry for the watershed extraction. The k-silon (2eqn) was selected as the fluid model; the discrete longitudinal coordinates were used as the radiation model; the cavity was set as a vacuum environment, with a density of 1.225 kg/m<sup>3</sup>, a Cp (specific heat) of 1006.43 J/(kg·K), a thermal conductivity of 0.0242 W/(m·K), a viscosity of 1.7894×10<sup>-5</sup> kg/(m·s), and a refraction of 1. The data were initialized in the calculation domain, and then the model was imported into Geometry for basin extraction. The computational domain was initialized with data and then the computation was performed, which converged after 500 iterations. Finally, the results of the simulation are then visualized and analyzed using the CFD-Post module.

### **Text S3 Catalysts synthesis**

The MgO/g-C<sub>3</sub>N<sub>4</sub> catalyst was prepared using the calcination process similar with the previous research <sup>1</sup>. Melamine (5 g) and MgO (0.5 g) were weighed and placed in a grinding bowl with an appropriate amount of ethanol for grinding. The ground mixture was dried in a drying oven at 80 °C overnight. Afterwards, the dried mixed samples were put into a muffle furnace for calcination. The temperature of the muffle furnace was set at 520 °C with a heating rate of 4 °C/min for 4 hours. The resulting yellow powdered composites were labeled as 0.5 MgO/g-C<sub>3</sub>N<sub>4</sub>. It was noted that the

synthesized catalysts were labeled with 0.5, 0.75, and 1.0 MgO/g-C<sub>3</sub>N<sub>4</sub> according to the mass of added MgO. The g-C<sub>3</sub>N<sub>4</sub> material was synthesized in the same manner using melamine as a control.

#### **Text S4 Photocatalytic degradation processes**

Toluene was used as the target pollutant in the photocatalytic degradation experiments. The catalysts were loaded onto the carriers before being placed in the carrier rack of the device for the next step of pollutant degradation. A fixed amount of 20 g of the composite catalyst was weighed into a beaker, and then a certain amount of thin alumina was added to improve the adhesion of the catalyst material, followed by 80 mL of ultrapure water. To improve the dispersion of the material in the ultrapure water, the configured suspension was sonicated for 20 min and then stirred on a rotary stirrer for 20 min. After that, the suspension is evenly applied to the cordierite carrier and then placed in the oven to dry overnight. Finally, after assembling the catalyst plates and the UV lamp, the air pump is turned on before each experiment so that the air path of the whole device can be kept stable during the real experiment to reduce experimental error. After the catalyst adsorption-desorption equilibrium, the UV lamp will be turned on for 20 minutes and then the degradation efficiency will be tested after the UV lamp operation remains stable. Each group of experiments will take one sample at the inlet and one at the outlet of the reactor to calculate the degradation efficiency and the experimental flow is shown in Fig. S1.

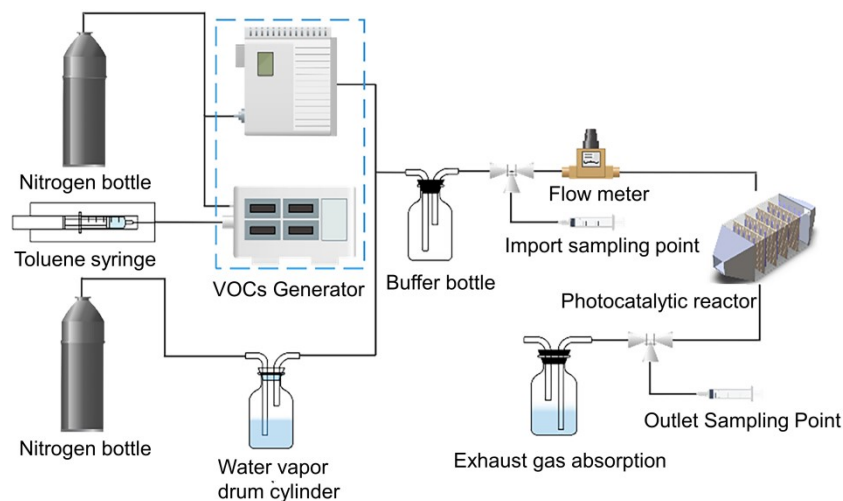


**Fig. S1** Experimental flow chart.

### **Text S5 Characterization**

X-ray diffraction (XRD) analysis was performed using a Bruker D8 Advance with a voltage setting of 40 kV and a scan range of  $10^{\circ}$  to  $80^{\circ}$ . The material surface morphology and elemental distribution were characterized using a scanning electron microscope (SEM, S-4800) and energy dispersive spectrometer (EDS). The elemental valence of the materials was determined using X-ray photoelectron spectroscopy (XPS). The types of functional groups and elemental bonding information in the samples were tested using Fourier infrared spectroscopy (FTIR, Vertex 70). Ultraviolet-visible diffuse reflectance spectroscopy (UV-vis) was used to probe the light absorption properties of the materials as well as the band gap variation. The photoelectrochemical test was performed using an electrochemical workstation. A certain amount of catalyst powder was weighed and dispersed in 1 mL of ethanol solution, and then a quantitative Nafion solution was added and sonicated to form a homogeneous suspension, which was then added dropwise onto ITO glass for testing. A standard three-electrode system

with a Pt electrode as the counter electrode and Ag/AgCl as the reference electrode was used for this test. The working conditions were a 300 W xenon lamp as the light source and 0.5 M Na<sub>2</sub>SO<sub>4</sub> solution as the electrolyte. DMPO was used as a trapping agent for •OH and •O<sub>2</sub><sup>-</sup>, and TEMP as a trapping agent for <sup>1</sup>O<sub>2</sub>. Electron paramagnetic resonance (EPR) was used to determine the active substances in the reaction process. Gas chromatography-mass spectrometry (GC-MS) Model 7890A-5975C, Agilent Technologies, USA. The starting temperature was kept at 35 °C for 4 min, and then increased to 220 °C at a rate of 17 °C/min for 5 min, the temperature of the gasification chamber was 250 °C, the temperature of the transmission line was 230 °C, the carrier gas was He, the flow rate of the carrier gas was 1.0 mL/min, and the injection volume was 2 mL without splitting. Mass spectrometry conditions: EI source; electron energy 70 eV, ion source temperature 230 °C, quadrupole 150 °C, scan mode Scan; scanning mass range 35-550u.

### **Text S6 DFT calculation**

First-principles calculations based on density functional theory (DFT) and plane wave pseudopotentials are performed using the Castep module<sup>2</sup>. The Perdew-Burke-generalized gradient approximation (GGA) was used for the exchange relation potential with a cutoff energy of 500 eV and a *k*-point sampling set of 3 × 3 × 1. To reduce interlayer interactions, the model was set to a vacuum layer of 20 Å and a 2 × 2 × 1 supercell model. The atoms were allowed to relax completely until the stress per atom was below 0.05 eV/Å, and the energy tolerance for electron density convergence was set to 10<sup>-5</sup> eV<sup>3</sup>. The adsorption energy is defined as follows :

$$E_{\text{ads}} = E_{\text{total}} - (E_{g\text{-C}_3\text{N}_4} + E_{\text{ob}})$$

Where  $E_{\text{total}}$ ,  $E_{g\text{-C}_3\text{N}_4}$  and  $E_{\text{ob}}$  are the total system energy, the individual g-C<sub>3</sub>N<sub>4</sub> energy and the energy of a target molecule, respectively.

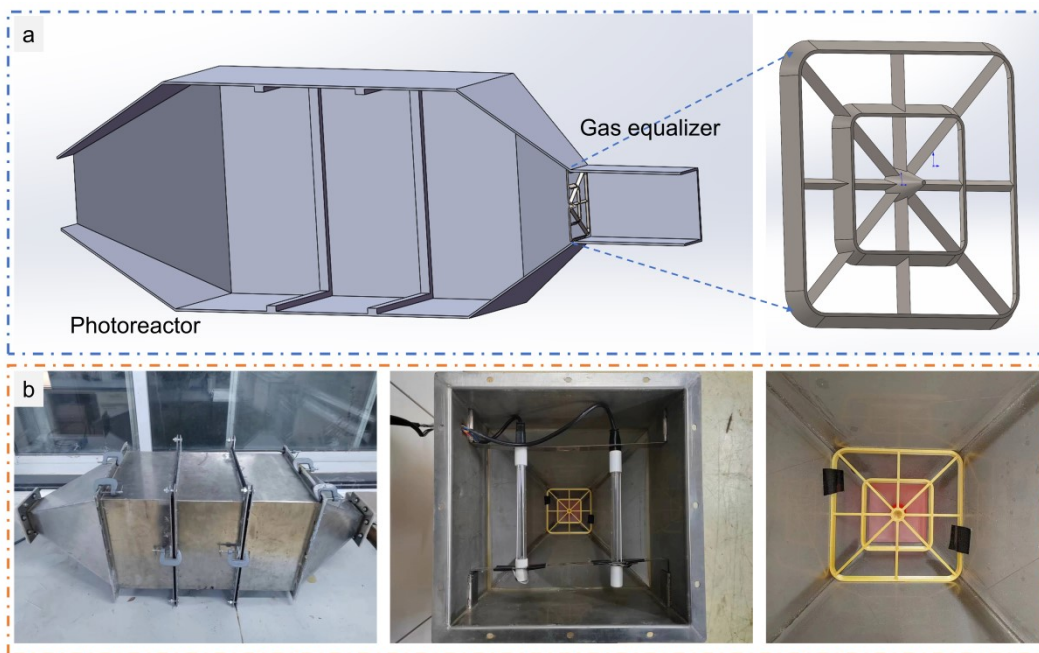


**Fig. S2** (a) model schematic and (b) actual photos of the photoreactor



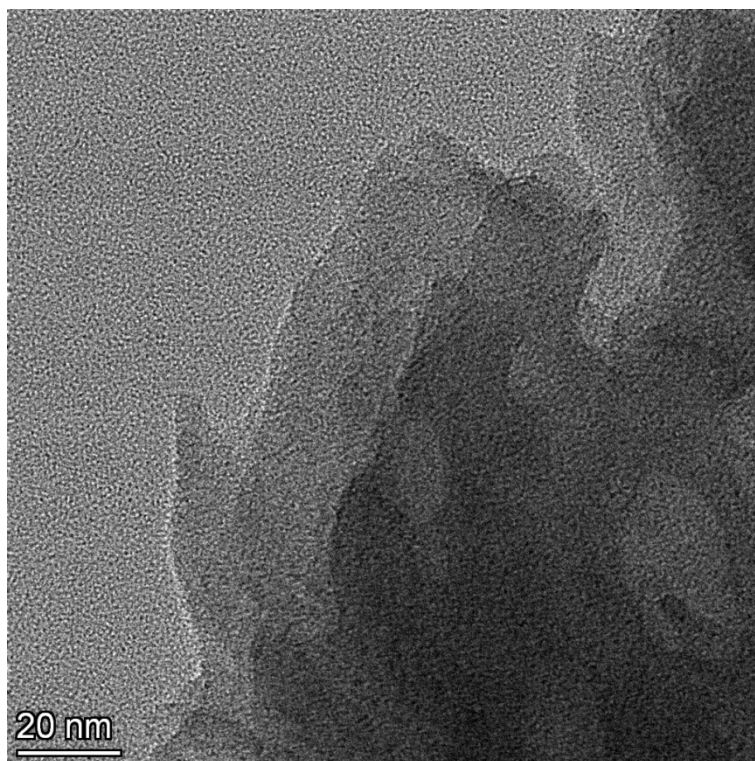


**Fig. S3** TEM of g-C<sub>3</sub>N<sub>4</sub>

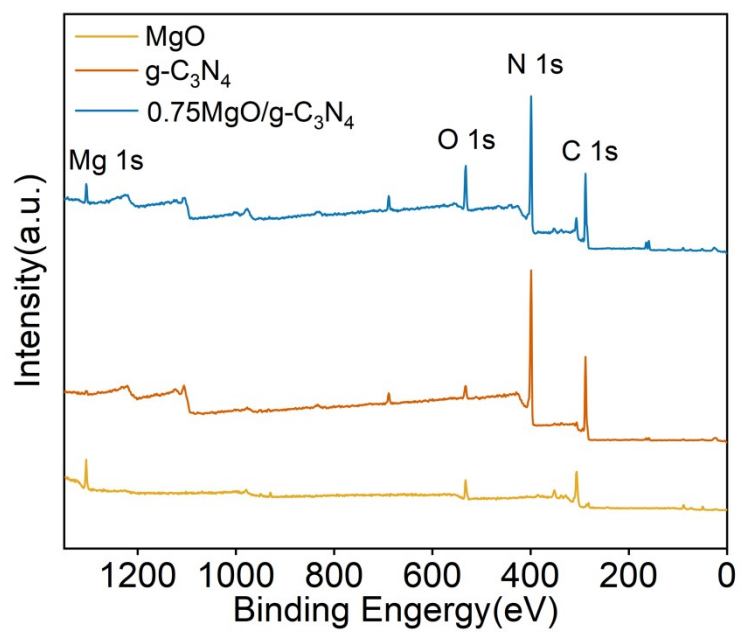


**Fig. S4** XPS image of the materials

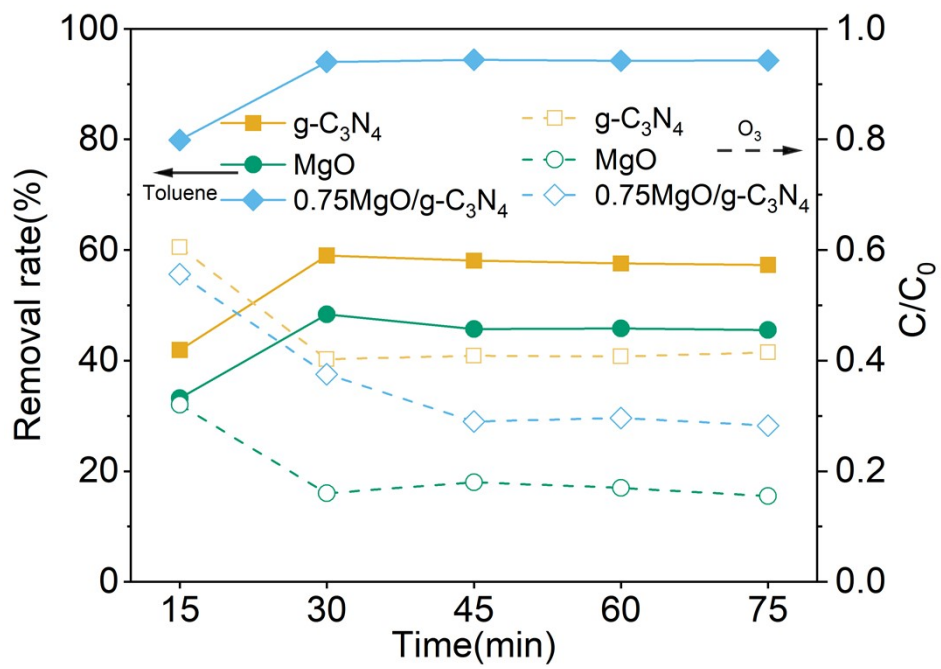


**Fig. S5** Degradation of toluene and O<sub>3</sub> at g-C<sub>3</sub>N<sub>4</sub>, MgO and 0.75MgO/g-C<sub>3</sub>N<sub>4</sub>. Conditions: Q<sub>in</sub>=17 L/min, C<sub>0</sub>=113.06 mg/m<sup>3</sup>, RH=61.2%.

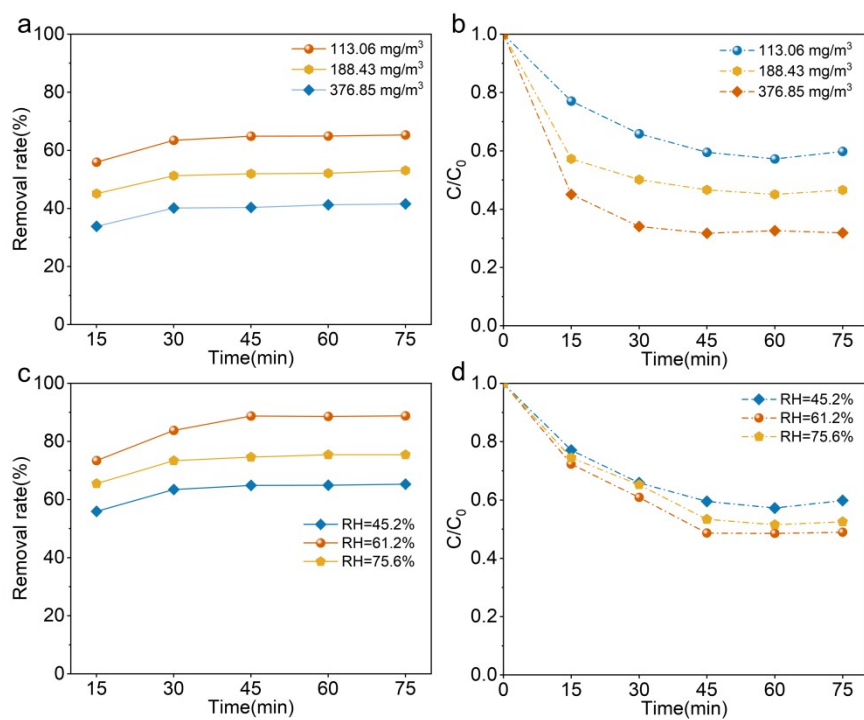


**Fig. S6** Degradation of (a) toluene and (b) O<sub>3</sub> at different initial toluene concentrations, Degradation of (c) toluene and (d) ozone at different relative humidity. Conditions: Q<sub>in</sub>=22 L/min, Lamps=4, C<sub>0</sub>=113.06 mg/m<sup>3</sup> except for (a, b), RH=45.2% except for (c, d).

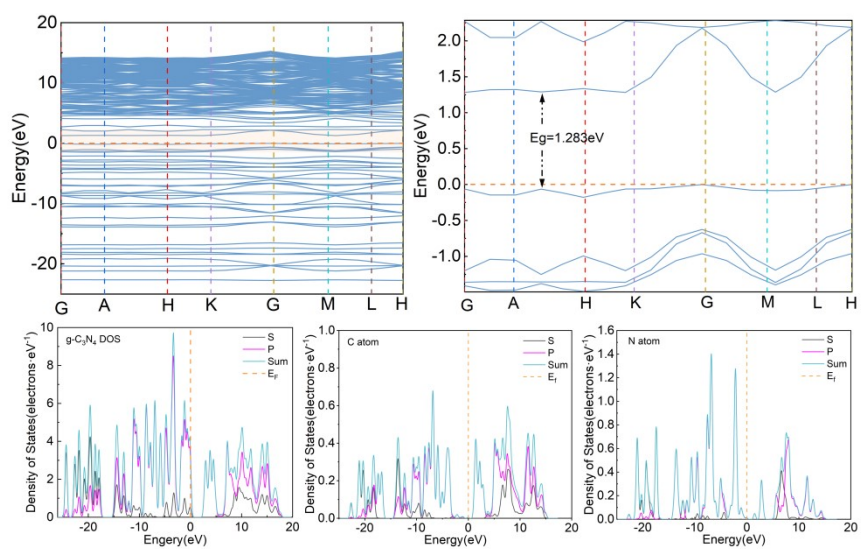


**Fig. S7**  $g\text{-C}_3\text{N}_4$  energy band structure and density of states diagrams.

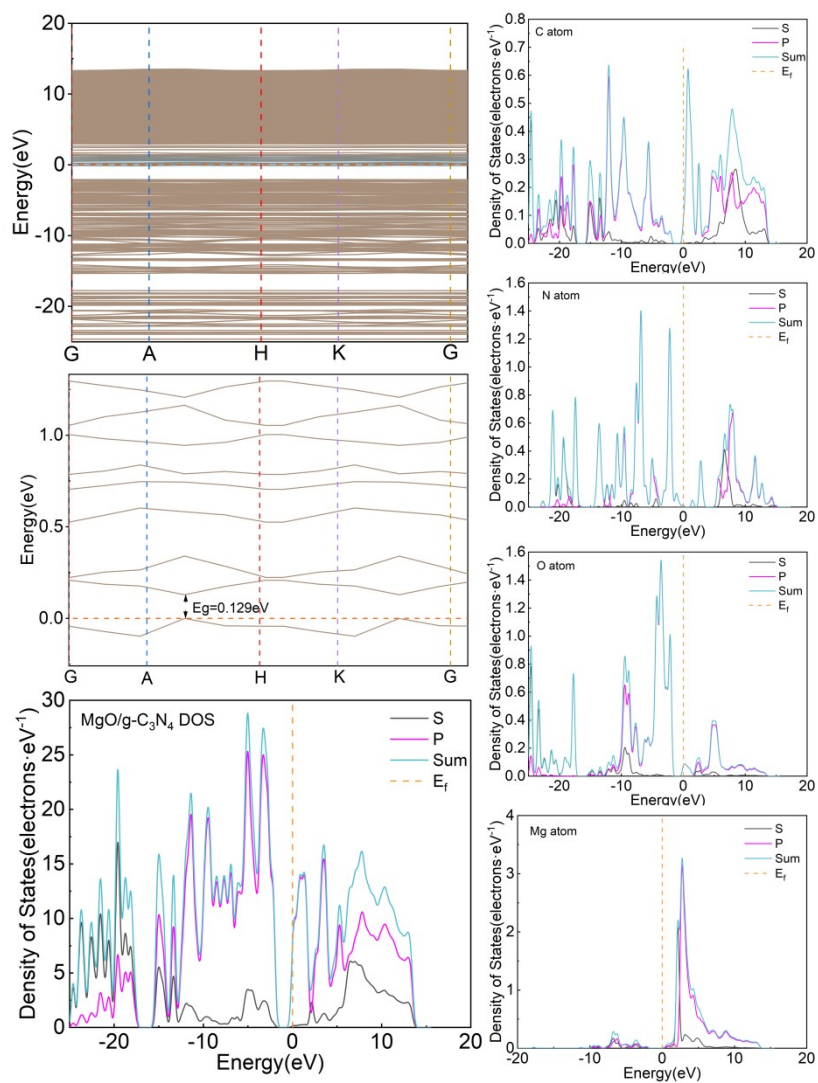


**Fig. S8** 0.75MgO/g-C<sub>3</sub>N<sub>4</sub> energy band structure and density of states diagrams.

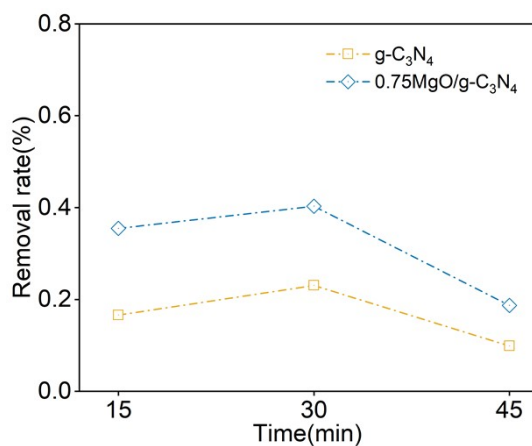


**Fig. S9** Adsorption of toluene and O<sub>3</sub> at g-C<sub>3</sub>N<sub>4</sub>, MgO and 0.75MgO/g-C<sub>3</sub>N<sub>4</sub>. Conditions: Q<sub>in</sub>=17 L/min, C<sub>0</sub>=113.06 mg/m<sup>3</sup>, RH=61.2%.

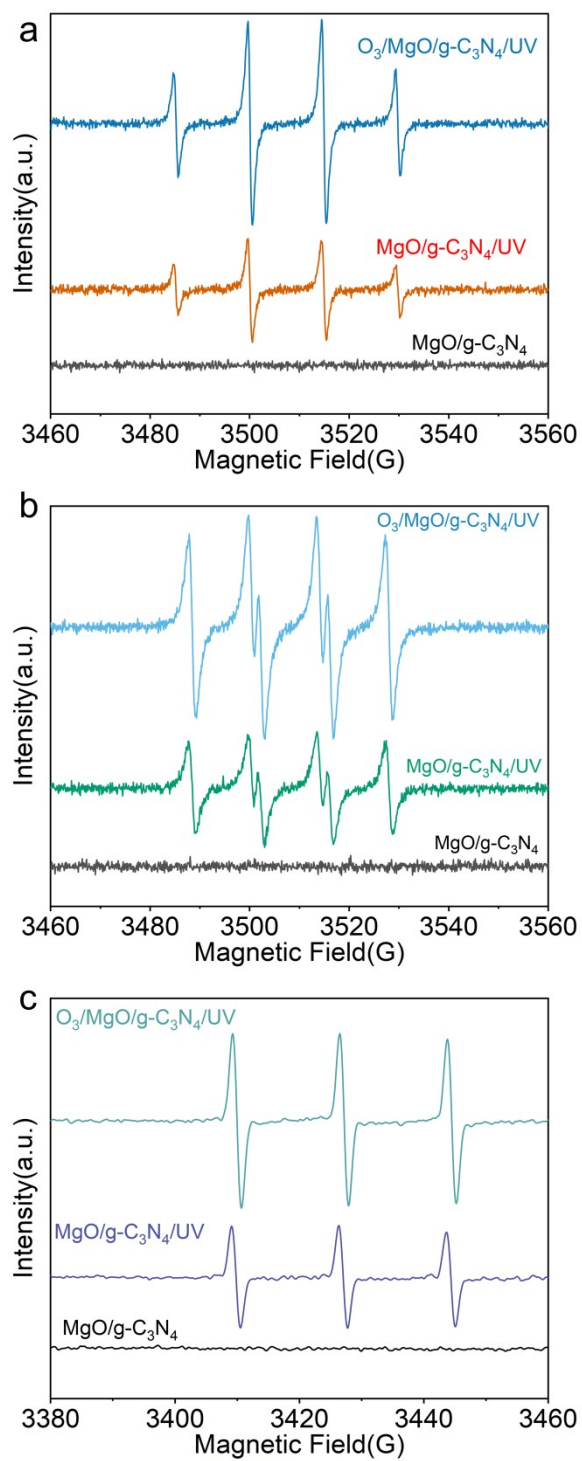


**Fig. S10** (a)  $\bullet\text{OH}$  spectrum, (b)  $\bullet\text{O}_2^-$  spectrum and (c)  $^1\text{O}_2$  spectrum of  $0.75\text{MgO}/\text{g-C}_3\text{N}_4$

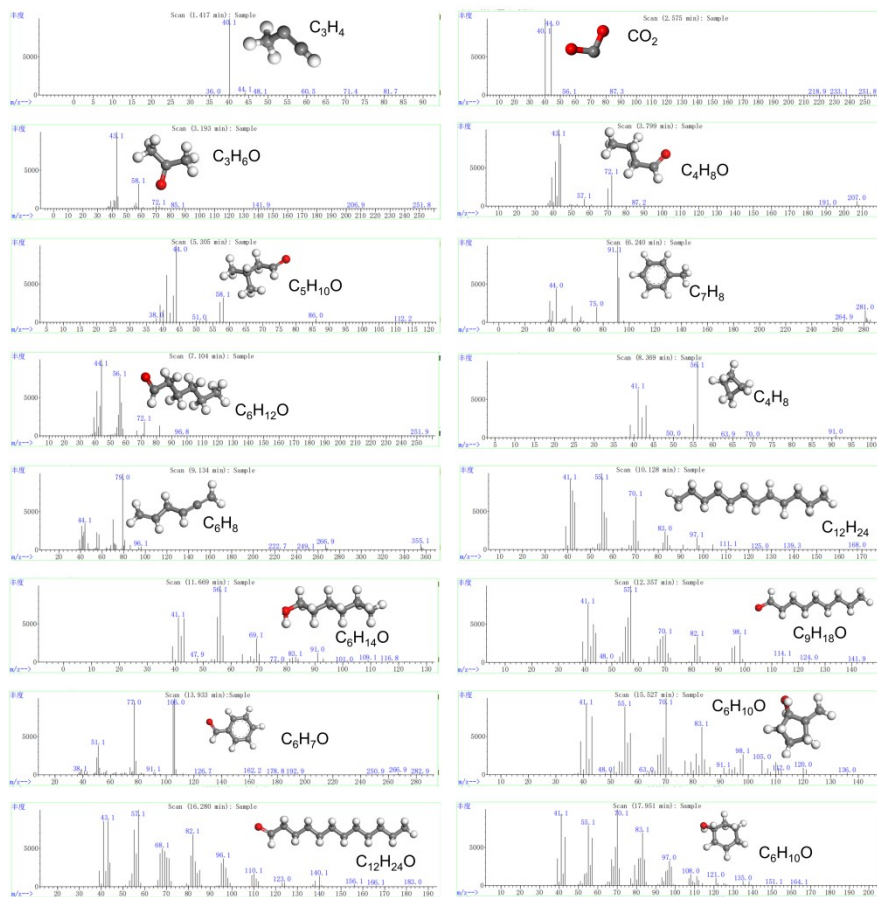


**Fig. S11** the spectra of degradation intermediates of toluene in full scan mode



## References

1. W. An, L. Tian, J. Hu, L. Liu, W. Cui and Y. Liang, *Applied Surface Science*, 2020, **534**, 147518.
2. M. Segall, P. J. Lindan, M. a. Probert, C. J. Pickard, P. J. Hasnip, S. Clark and M. Payne, *Journal of physics: condensed matter*, 2002, **14**, 2717.
3. G. Gao, Y. Jiao, F. Ma, Y. Jiao, E. Waclawik and A. Du, *Physical Chemistry Chemical Physics*, 2015, **17**, 31140-31144.